11 Particle physics with CMS

E. Aguiló, C. Amsler, S. de Visscher, M. Ivova, B. Millán Mejías, P. Otyugova, M. Rebero‡, P. Robmann, and A. Schmidt,

V. Chiochia, C. Favaro, H. Snoek, S. Tupputi, and M. Verzetti

in collaboration with: the CMS Collaboration
‡ CERN summer student

In 2011 the Large Hadron Collider delivered an integrated luminosity of 5.7 fb^{-1} at 7 TeV (Fig. 11.1) while at most 1 fb^{-1} had been expected at the beginning of the run operation back in March. During this long run CMS recorded 5.2 fb^{-1} of data with its subdetectors performing at an efficiency of 98.5%. The silicon barrel pixel detector, the innermost component of the CMS experiment ,was developed in and commissioned by our group (in collaboration with PSI). It allows a precise reconstruction of charged particle tracks and the identification of secondary vertices from long-lived particles. This device is crucial for our research using b-quarks. Details can be found in earlier annual reports.

More than one hundred refereed journal articles have been published by the CMS collaboration in 2011. One of us (V. C.) co-chaired the B-physics analysis group, that has so far released twelve journal articles on quarkonium, B hadron decays and b-quark production measurements. H. S. convened the pixel calibration and reconstruction group, S. d.V. coordinated the simulation in the standard model (SM) physics group. Here we report on the analysis results achieved by the Zurich group on heavy baryons, B_s decays, Higgs searches in τ-lepton pairs and $b\bar{b}$ angular correlations.

11.1 Study of Λ_b and Σ_b

The spectroscopy of b-baryons provides valuable information to test QCD models. Baryon production mechanisms and dynamics of heavy quark decay can be studied from polarization measurements in b-baryon decays. Our group is studying the Λ_b polarization in the decay $\Lambda_b \to J/\psi\ (\to \mu^+\mu^-)\Lambda(\to p\pi^-)$ (Fig. 11.2). To select clean Λ_b candidates large transverse momenta and narrow windows around the Λ and J/ψ masses are chosen, and tight vertex cuts chosen for the daughter particles. The $J/\psi\ \Lambda$ invariant mass distribution is

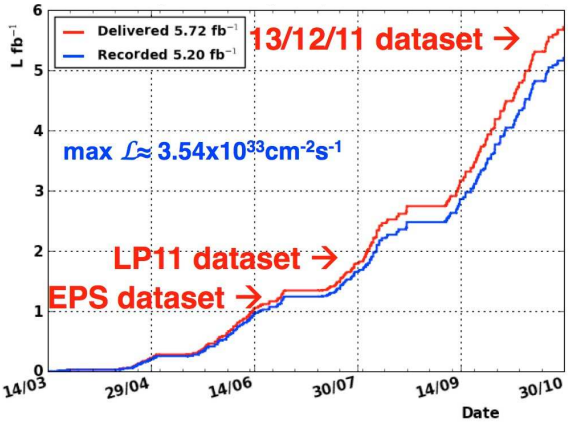

FIG. 11.1 – *Integrated luminosity in the 2011 LHC run at $\sqrt{s}$ = 7 TeV.*

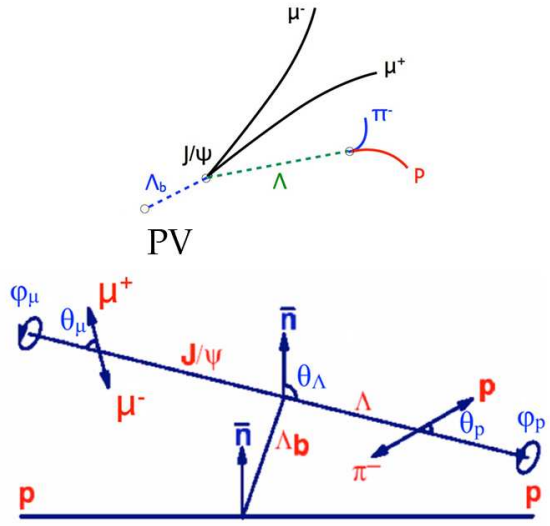

FIG. 11.2 – *Decay $\Lambda_b \to J/\psi\ (\to \mu^+\mu^-)\Lambda(\to p\pi^-)$ and angles used in the Λ_b polarization analysis.*

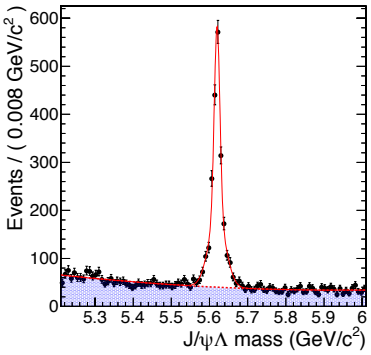

FIG. 11.3 – *J/ψ Λ invariant mass distribution with Λ_b fit (red).*

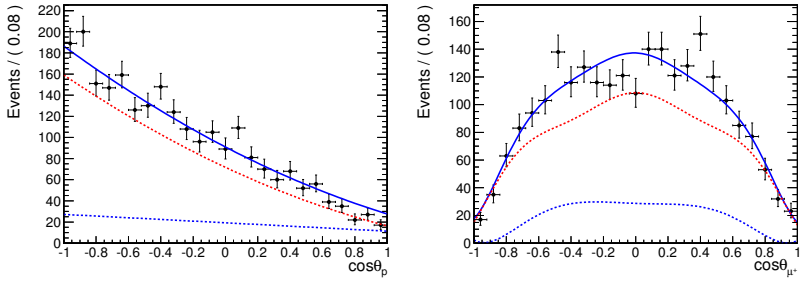

FIG. 11.4 – *$\cos\theta_p$ (left) and $\cos\theta_\mu$ (right) distributions in the Λ and J/ψ rest frames with the results of a multidimensional likelihood fit (blue line). The dashed lines show the fits to the Λ_b signal (red) and the background contribution (blue).*

shown in Fig. 11.3 from 5 fb^{-1} of integrated luminosity, leading to 1929 ± 54 Λ_b-baryons.

We use the angles θ_Λ, θ_p and θ_μ, the polar angles of the Λ, the proton and the μ^+ in the respective rest frames of Λ_b, Λ and J/ψ (Fig. 11.2). The Λ_b polarization manifests itself by a slope in the $\cos\theta_\Lambda$ distribution that can be extracted by analyzing the angular correlations between the daughter particles [1]. The distortions in the angular distributions due to acceptance and cuts are taken into account by Monte Carlo simulation. Sidebands of the Λ_b mass peak are used to estimate the contamination from background. A maximum likelihood fit is then performed. Figure 11.4 shows for instance a preliminary distribution of cosθ_p and cosθ_μ together with fits. Work on this analysis is in progress [2].

The Λ_b candidates are also used to reconstruct the four states $\Sigma_b^{(*)\pm} \to \Lambda_b\pi^\pm$ where the Σ_b or Σ_b^* decays strongly at the primary vertex. Tight requirements are applied on the soft pion to suppress the large combinatorial background from other tracks. Figure 11.5 shows the distributions of the Q-values of the decays. The reconstructed candidates can be used to measure Σ_b cross-sections relative to those for Λ_b.

11.2 Observation of a new strange bottom baryon

The $\Xi_b^-(5790)$, a *dbs*-baryon, and its Ξ_b^0 isospin partner, a *ubs*-baryon, have been observed at the Tevatron [3]. However, there are two other ground state pairs of baryons in the SU(4) classification, the Ξ_b' with spin 1/2 and the Ξ_b^* with spin 3/2, which can both be negatively charged (*dsb*) or neutral (*usb*). Theory (e.g. ref. [4])

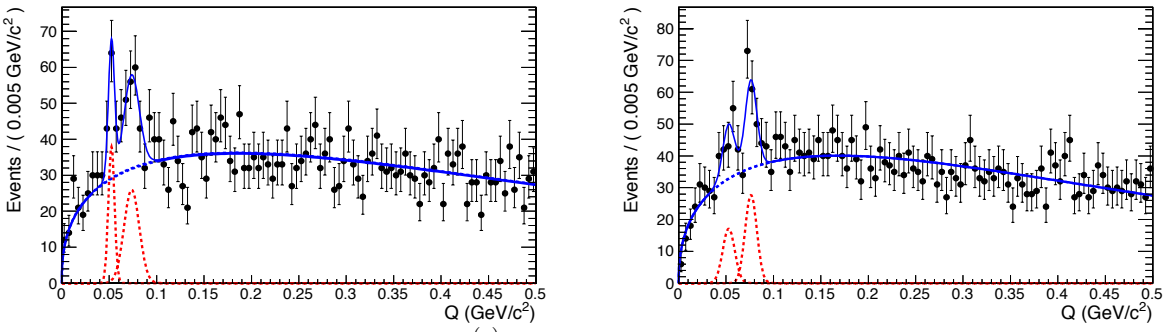

FIG. 11.5 – *Q-value distributions for the $\Sigma_b^{(*)}$ decays, where $Q = M(\Lambda_b\pi) - M(\Lambda_b) - M(\pi)$. Left: Σ_b^+ and Σ_b^{*+}. Right: Σ_b^- and Σ_b^{*-}.*

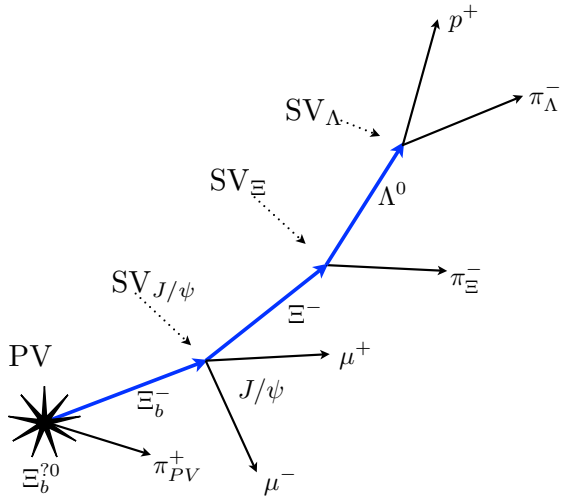

FIG. 11.6 – *Decay chain of the new baryon (marked $\Xi^{?0}$ at the primary vertex PV). Charge conjugation (baryons and antibaryons) is implicitely assumed.*

predicts the mass difference between the Ξ'_b and the Ξ_b to be smaller than the mass of the pion, which forbids the decay $\Xi'_b \to \Xi_b\pi$. In contrast, the Ξ^*_b would be heavy enough to decay (strongly) into the Ξ_b by pion emission.

We have observed a new *usb*-baryon decaying into $\Xi^-_b\pi^+$ using 5.0 fb^{-1} of data. We reconstruct the decay $\Xi^-_b \to J/\psi\ \Xi^-$, with $J/\psi \to \mu^+\mu^-$ and $\Xi^- \to \Lambda\pi^-$, $\Lambda \to \pi^- p$ (Fig. 11.6). The events were collected with a trigger requiring a secondary vertex (SV) displaced from the primary (PV), from which two muons emerge with transverse momenta larger than 3 GeV/c and invariant mass compatible with the J/ψ (for details on additional selection cuts see ref. [5]). The Λ (or $\overline{\Lambda}$) decays into two opposite charges. The higher momentum track is assumed to be the proton. The two tracks are required to form a vertex displaced from the beamline. The candidate Ξ^- (or $\overline{\Xi^-}$) is reconstructed by combining the Λ with an additional track. A kinematic vertex fit is performed in which the track is assumed to be a pion and the Λ mass constrained to its known value. Figure 11.7 shows the $\Lambda\pi^-$ invariant mass distribution with the Ξ^- signal. The Ξ^-s are then combined with the J/ψ with a kinematic vertex fit, constraining the Ξ^-- and J/ψ-masses to their known values. The resulting $J/\psi\ \Xi^-$ invariant mass distribution with the Ξ^-_b peak (108 ± 14 events) is displayed in Fig. 11.8 after all selection cuts. The measured mass is in good agreement with the known value.

We then combine the Ξ^-_b baryon with an additional track assumed to be a π and emerging from the PV with charge opposite to the π from Ξ^- (or $\overline{\Xi^-}$) decay, and search for narrow resonances in the mass difference distribution (Fig. 11.9). We observe 29 candidates (with a background of 6.6 ± 2.6) and obtain a mass of 5944.9 ± 2.8 MeV. This state is thus 154 MeV heavier than the spin 1/2 Ξ^-_b. Unfortunately the data sample is too small to determine its spin from the decay angular distributions. According to predictions this new baryon would be the Ξ^{*0}_b with spin 3/2.

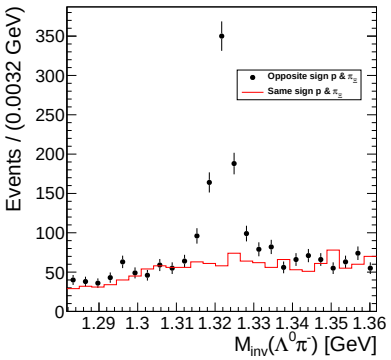

FIG. 11.7 – $\Lambda\pi^-$ *invariant mass distribution showing the* Ξ^-.

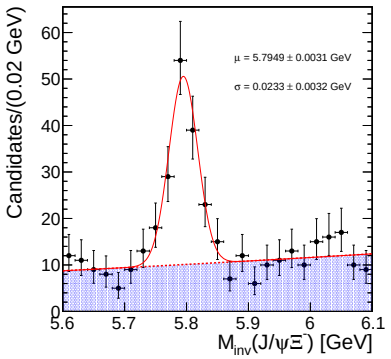

FIG. 11.8 – $J/\psi\ \Xi^-$ *invariant mass distribution showing the* Ξ^-_b *signal with fit.*

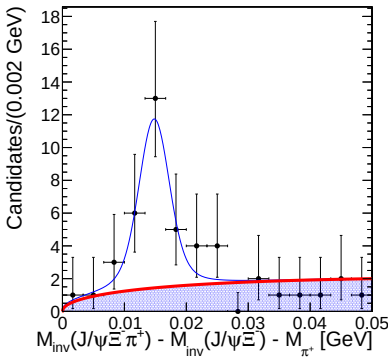

FIG. 11.9 – *Q-value distribution of the reaction* $\Xi^-_b\pi^+ \to J/\psi\ \Xi^-\pi^+$ *showing the new* Ξ^{*0}_b *with fits.*

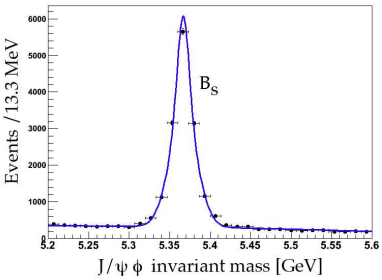

FIG. 11.10 – *J/ψ ϕ invariant mass showing the B_s (15'000 events).*

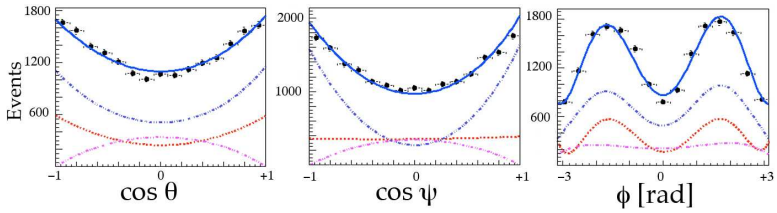

FIG. 11.11 – *Measured angular distributions. The dark blue line is the fit, the dotted blue line is the CP-even component, the magenta line the CP-odd component. The red curve shows the background contribution.*

11.3 Lifetime of the B_s-meson

We are measuring the width difference $\Delta\Gamma_s = \Gamma_L$ - Γ_H of the two CP-Eigenstates of the B_s-meson, B_L (CP = +1) and B_H (CP = -1) in the decay $B_s \to J/\psi\ (\to \mu^+\mu^-)\ \phi(\to K^+K^-)$. Three angles are needed to describe this decay. The angles θ and ϕ give the flight direction of the μ^+ in the J/ψ rest frame while ψ is the azimuthal angle of the K^+ with respect to the flight direction of the J/ψ. Since the B_s is pseudoscalar, while the J/ψ and ϕ are vectors, the angular momentum between the two decay products is $L = 0$, or 2 for B_L and $L = 1$ for B_H. Hence the angular distributions are different for the two states (for details see e.g. ref. [6]).

During 2011 we collected 15'000 $B_s \to J/\psi(\to \mu^+\mu^-)\phi(\to K^+K^-)$ events at $\sqrt{s} = 7$ TeV with an integrated luminosity of 4.6 fb^{-1}. Our B_s are "untagged", which means that we do not distinguish between B_s and $\overline{B}_s$. The muons pairs are selected with a trigger on displaced J/ψ decay point with respect to the primary vertex. Various cuts are applied, in particular the muons and kaons are required to have transverse momenta larger than 4, respectively 0.7 GeV/c. An additional cut on the decay length reduces the prompt J/ψ background from the primary vertex. The $B_s \to J/\psi\ \phi$ peak is shown in Fig. 11.10.

Side band subtraction is applied to determine the contribution from background. Efficiency and acceptance corrections are calculated by Monte Carlo simulation. The results of the likelihood fit taking into account the mass, decay length and angular distributions are shown in Fig. 11.11. The dark blue line is the fit, the dotted blue (magenta) line is the contribution from the CP even (odd) component. Fitted mass and mean life are in excellent agreement with the known values (5366 MeV and 1.43 ps). This work is still in progress [7] and we obtain a preliminary value for $\frac{\Delta\Gamma_s}{\Gamma_s}$ of 0.107 $\pm$ 0.019, where the error is statistical only. This is compatible with the prediction from the SM: 0.147 $\pm$ 0.060.

11.4 Searches for the Higgs boson in $\tau^+\tau^-$ decays

An important goal of the LHC physics program is to ascertain the mechanism of electroweak symmetry breaking, through which the W and Z^0 bosons obtain mass, while the photon remains massless. In the SM this is achieved via the Higgs mechanism which predicts the existence of a scalar Higgs boson. The minimal supersymmetric standard model (MSSM) contains two Higgs doublets, giving rise to five physical states: a light neutral CP-even state (h), a heavy neutral CP-event state (H), a neutral CP-odd state (A), and a pair of charged states ($H^\pm$).

A search for the neutral Higgs boson decaying into τ-pairs was performed using an integrated luminosity of 4.6 fb^{-1} [8]. Three independent τ-pair final states were studied with one (or both) τ-leptons decaying leptonically. The distribution of the τ-pair invariant mass for all channels combined is shown in Fig. 11.12 for the MSSM search. The spec-

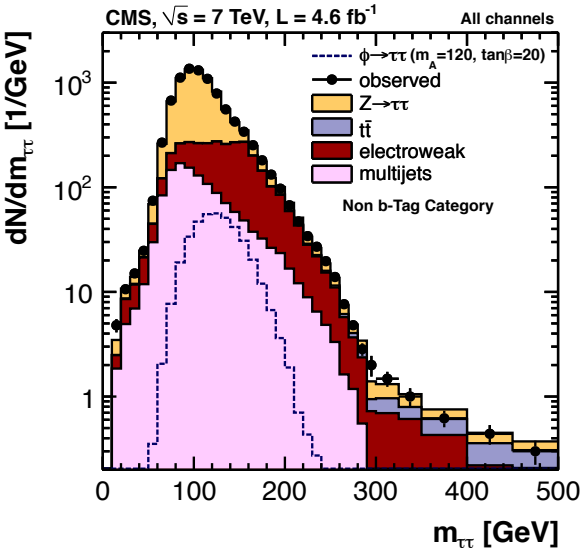

FIG. 11.12 – *τ-pair invariant mass distribution in the MSSM Higgs boson search for data (full dots) and simulation (stacked histograms).*

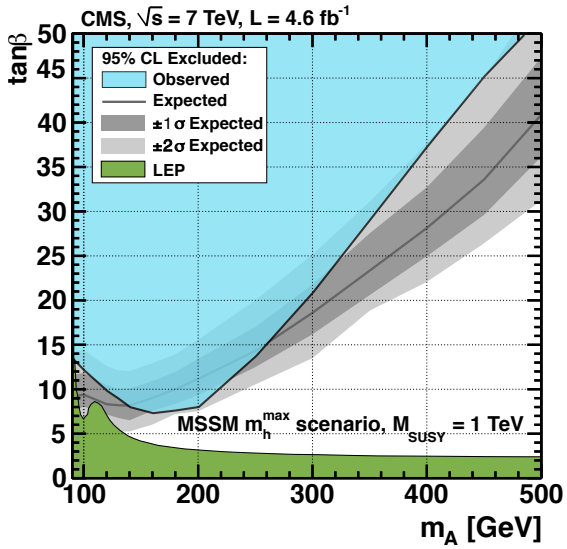

FIG. 11.13 – *Region in the* $\tan\beta$ *vs.* m_A *parameter space excluded at 95% CL in the MSSM* m_h^{max} *scenario.*

tra show no evidence for a Higgs boson in both MSSM and SM searches. Upper bounds (95% CL) on the Higgs boson cross section times the branching fraction into τ-pairs are shown in Fig. 11.13. We exclude a Higgs boson with mass $m_H = 125$ GeV with a production cross section 4.4 times that predicted by the SM. The MSSM search excludes previously unexplored regions of the parameter space, reaching as low as $\tan\beta = 7.1$ at $m_A = 160$ GeV.

These Higgs searches rely on the precise estimate of the reconstruction efficiency for the τ hadronic decay, which was measured by our group using a *tag-and-probe* technique [9]. This method exploits the decay $Z^0 \to \tau_\mu \tau_{\rm had}$, where τ_μ is a τ decaying into a μ while $\tau_{\rm had}$ represents a τ decay into charged hadrons. The events are required to have exactly one isolated μ and a jet of opposite sign. The events are divided into those surviving a tight cut and those failing the cut, and a simultaneous fit of the visible τ-pair invariant mass is performed in the signal and background regions (Fig. 11.14). The measured τ identification efficiency is typically 60% and agrees well with Monte Carlo simulation. The overall precision of the measurement is 6% (including systematic errors). With the higher instantaneous luminosity in 2012 we will further quantify the performance of hadronic τ reconstruction in an environment characterized by a larger number of simultaneous pp collisions. We are also responsible for the development of the software monitoring the performance of τ-lepton identification.

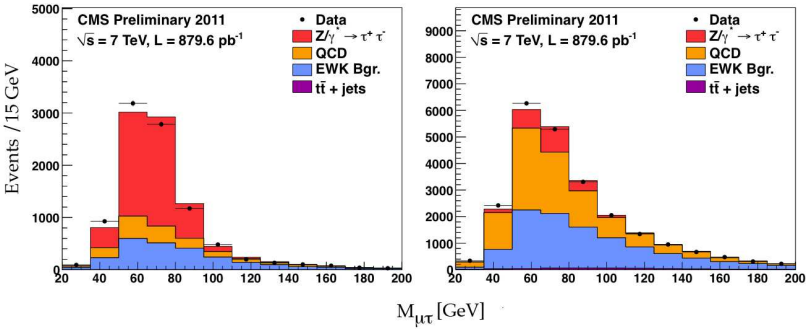

FIG. 11.14 – *τ-pair invariant mass distribution with various signal and background processes for events passing the identification cut (left) and for those failing the identification cut (right).*

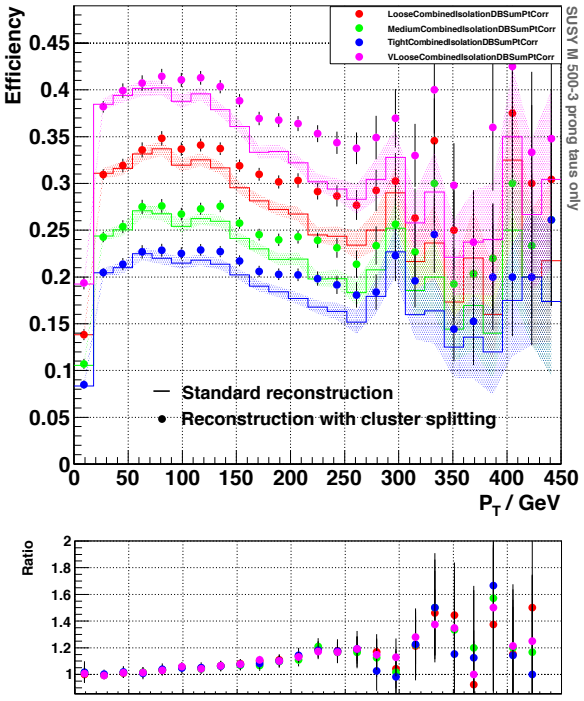

FIG. 11.15 – *τ identification efficiency as a function of transverse momentum for Higgs decays. The dots show the improved hit reconstruction based on pixel hit splitting compared to the standard case (histograms). The colors represent the various τ identification procedures. The lower plot shows the relative improvement.*

11.5 Improvements to the pixel hit reconstruction

We are developing a novel hit reconstruction technique to improve the spatial disentanglement in a dense charged track environment. The implementation of this technique in the CMS software will affect all analyses that depend on the reconstruction of high energetic jets, such as b or τ jets. A fraction of 65% of the τ decay hadronically. The transverse momentum of the τ being large compared to its mass, the tracks in the jet are close to each other. Therefore, excellent spatial resolution is needed for τ reconstruction.

A significant amount of the hadronic τ decays are produced in three charged tracks accompanied by the (invisible) neutrino. The higher the τ momentum, the more collimated the three tracks, which makes them at some point inseparable. In the innermost pixel layer this effect starts to occur for opening angles between the two trajectories of about 5 mrad. For a typical 3-prong τ decay this corresponds to a transverse momentum of 150 GeV/c. The merging of clusters deteriorates the measurement of the particle trajectories and the reconstruction of the τ-lepton.

The charge measured for each cluster, together with an estimate of the track impact angle, can be used to discriminate merged clusters from isolated clusters. We have developed an algorithm for splitting merged pixel clusters, now deployed in the CMS software. The performance improvement in the τ reconstruction was verified on a simulated sample of 500 GeV MSSM Higgs bosons decaying into τ-pairs. Figure 11.15 shows the τ identification efficiency for 3-prong decays as function of τ transverse momentum. Our algorithm improves the identification efficiency by ∼20% for $p_T(\tau) > 200$ GeV/c for the four τ identification procedures in CMS (Fig. 11.15, bottom).

11.6 Studies of B hadron correlations associated to Z^0 bosons

A measurement of the b-quark production associated with a Z^0/γ^* is an important test of QCD and is of great experimental relevance for various searches. The process constitutes a background to the SM Higgs production decaying to $b\bar{b}$, associated with vector bosons. In addition, in models with extended Higgs sector (such as the two-Higgs doublet models), a discovery channel would be $\phi_1 \to Z^0\phi_2$ with $\phi_2 \to b\bar{b}$, where $\phi_{1,2}$ are neutral Higgs bosons. Finally, the description of the b-quark dynamics remains difficult, in particular in the soft-collinear region, where the gluon splitting contribution to $q\bar{q}$-pairs is not well known.

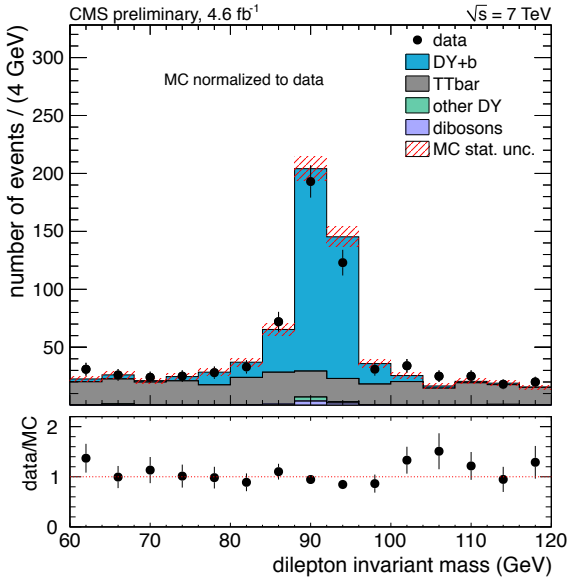

FIG. 11.16 – *Dilepton invariant mass distribution.*

Our group has performed a measurement of the normalized differential cross-section $pp \to Z^0/\gamma^* + b\bar{b}$ as a function of B-hadron angular separation [10] for an integrated luminosity of 4.6 fb^{-1}. Leptonic decays of the Z^0 into two leptons (e or μ) of opposite charges are selected (Fig. 11.16). The B-hadron pairs are identified by the Inclusive Vertex Finder (IVF) algorithm, based on the reconstruction of displaced secondary vertices from B decays,

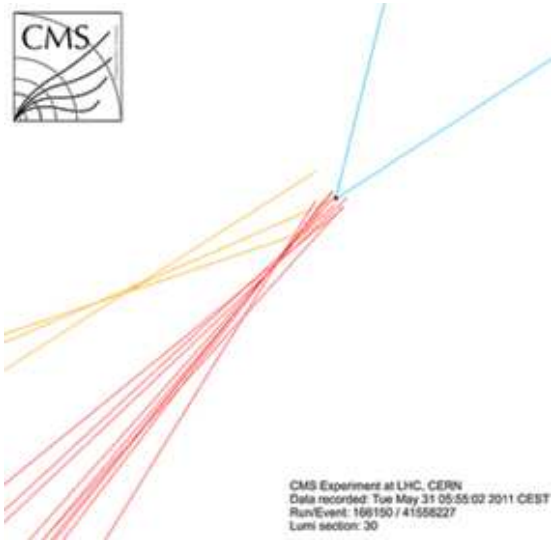

FIG. 11.17 – *Event with two displaced vertices from B-hadron decays (red and yellow tracks) and two leptons from a Z^0 boson (blue tracks).*

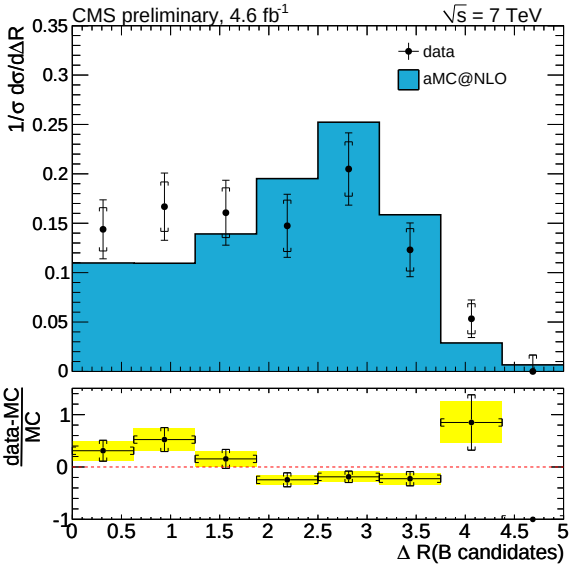

FIG. 11.18 – *Normalized production cross section as a function of the angular variable $\Delta R = \sqrt{\Delta\eta^2 + \Delta\phi^2}$. The measured distribution (solid dots) is compared to* `aMC@NLO` *prediction.*

independently on jets. This allows to resolve B-hadron pairs even at small opening angles (see Fig. 11.17) for which decay products merge into single jets, the standard b-jet tagging techniques then becoming useless.

The observed distribution is compared to the the NLO expectation obtained with `aMC@NLO` (Fig. 11.18). The data agree reasonably well with simulation within experimental errors, although data suggest a flatter angular distribution at small ΔR. Additional investigations and larger data samples in 2012 will help establishing which theoretical model provides the best description of the data [11].

We are also working on the implementation of the jet matching techniques for the `MADGRAPH` Monte Carlo simulation which will allow to efficiently produce exclusive samples of $pp \to Z^0/\gamma^* + b\bar{b}$ events with additional partons. We are implementing the simulation of massive b-quarks in `MADGRAPH`.

Our group has furthermore improved the b-jet identification in the High Level Trigger (HLT). The reconstruction of the primary vertex is crucial for the application of b-tagging algorithms. To limit CPU time the standard HLT reconstruction per-

forms only a fast 1D estimate of the primary vertex position in the direction of the beam axis, while the coordinates of the online beam spot are used as estimates for the transverse vertex position. The efficiency of the trigger can be improved with an event-by-event estimate of the 3D vertex position at the trigger level. We have assessed the performance of the 3D primary vertex reconstruction using a simulated sample of jet events and an average event pileup of 10, and have established that the algorithm can be successfully applied at trigger level.

[1] M. Kramer and H. Simma, Nucl. Phys. **B 50** (1996) 125.

[2] M. Ivova Rikova, PhD-thesis, Universität Zürich (in preparation).

[3] V. M. Abazov *et al.*, Phys. Rev. Lett. **99** (2007) 052001; T. Aaltonen *et al.*, Phys. Rev. Lett. **99** (2007) 052002.

[4] M. Karliner *et al.*, arXiv:0706.2163 [hep-ph] (2007).

[5] E. Aguiló, CMS-PAS-BPH-12-001 (to be published).

[6] L. Wilke, PhD-Thesis, University of Zurich (2009).

[7] B. Millán Mejías, PhD-thesis, Universität Zürich (in preparation).

[8] CMS Collaboration, submitted to Phys. Lett. B, prep. arXiv:1202.4083 [hep-ex] (2012).

[9] M. Verzetti, PoS (EPS-HEP2011) 417 (2011).

[10] CMS Collaboration, CMS-PAS-EWK-11-015 (to be published).

[11] C. Favaro, PhD-thesis, Universität Zürich (in preparation).